Polarimetric Classification and Decomposition of Synthetic Aperture RADAR Data using SNAP

[1]Ben Pietersen and [2]Ryan Davidson,
[1]Faculty of Engineering, Built Environment & IT, University of Pretoria
[2]Department of Geography, Geoinformatics & Meteorology, University of Pretoria, Pretoria, South Africa

Abstract: In this report Wishart Classification and H-⊛ decomposition of dual-polarization polarimetric Synthetic Aperture Radar (SAR) data was used to determine and classify different ground properties in an observed region in the Gauteng province of South Africa. The image processing application used to perform the analysis was SNAP[1]and the acquired observational area for classification was obtained by the Sentinel-1 satellite constellation. The objective of the report is to determine whether Wishart Classification and H-⊛ decomposition techniques can accurately classify and determine specific land features within the Vaaldam region in order to determine the best area for agricultural land development and zoning. This identification process is important as there is a steadily growing population in the Southern African Developing Countries(SADC) with an increasing demand for food and agricultural real estate [2]. The H-⊛ parameter combined with the Wishart classifier were used to segment the different zones of the SAR image in order to accurately classify the region. The classification and elevation map were used to determine the suitability of the possible future agricultural developments.

Keywords: *Synthetic Aperture Radar (SAR), Classification; Decomposition, SNAP, Vaaldam, South Africa, H-Alpha, Agriculture Planning*

I. INTRODUCTION

Growing levels of urbanization lead to more infrastructure being built and with that, an increasing urban sprawl. There is thus an increasing need for terrain mapping and classification of areas in order to aid the layout and planning of cities and agricultural zoning[3]. The classification and mapping of terrain is becoming more accessible as there is a continuous increase in open-source tools and publicly available remotely sensed data. The use of Sentinel-1A's Synthetic Aperture RADAR is a powerful tool in the arsenal of remote sensing and has many capabilities and advantages. Sentinel-1A's SAR system is an active RADAR sensor that does not require an external energy source for the acquisition of its data, the specific wavelengths of the microwave region which are used by the system are able to penetrate the atmosphere with little distortion and therefore can be used for multiple purposes. The raw Sentinel 1 image data was acquired from Copernicus Open Access Hub[4]and extracted before image processing and classification could begin. The Wishart Classification and H-⊛ decomposition of the dual-polarization polarimetric SAR data was used to classify the impervious surfaces, bare soil, vegetation and water of the subject area which can be seen below in Figure 1.
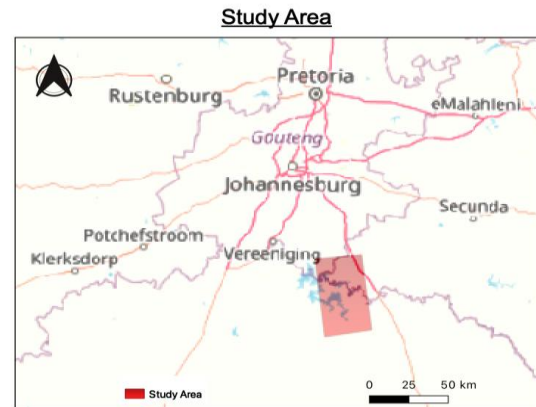

Figure 1: The Subject area is a portion of the Vaaldam which spans across the Gauteng, Freestate and Mpumalanga provinces.

II. MATERIALS AND METHODS

There are several methods commonly used to go about the decomposition and classification of SAR data. These methods include Singular Value Decomposition (SVD), which is a purely computational and context free mathematical method and Satellite Image-Time Series (SITS) which tracks changes in ground features over time. We made use of the H-α (H-Alpha) decomposition and Wishart classification technique[5]in order to determine if it is a valid method for mapping and classifying regions using FOSS (free and open-source) applications.
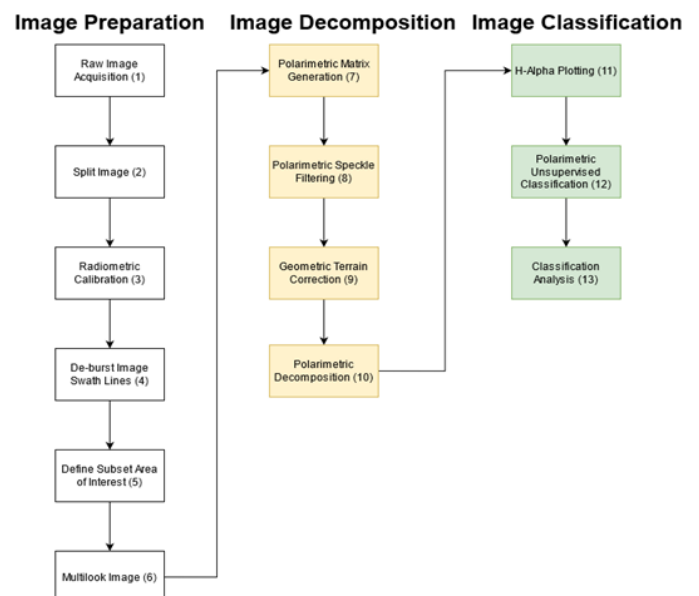
A. Image Processing Workflow

Figure 2*:* Visual representation of the workflow involved in polarimetric decomposition and classification using SNAP.

B. Software and Data

1. Data

Sentinel-1A

- S1A_IW_SLC__1SDV_20210626T164649_2021062
6T164716_037988_047BD5_2490.zip

The raw image used was from the Sentinel-1A platform (S1A), in its Interferometric Wide Swath (IW) acquisition mode. The product type is a Single Lookup Complex (SLC) which has VH and VV components and is unprocessed. All subsequent files and processing steps were derived from this base image set [4].

2. Software

- SNAP 8.0.5 - Constituents
  - SNAP Desktop Implementation Version: 8.0.5
  - SNAP Engine Implementation Version: 8.0.5
  - JRE: OpenJDK Runtime Environment 1.8.0
  - JVM: OpenJDK 64-Bit
- Blender 2.8 beta
- Google Earth Pro 7.3.4.8573 (64-bit)
- Windows 10 Home OS Build 18363.1556

3. Hardware

- AMD Ryzen 7 3700U with Radeon Vega Mobile Gfx ~2.30 GHz
- 32GB RAM (29.9GB usable)
- 256GB SSD (System Partition), 1TB HDD

C. Methodology

The following section explains the steps followed in order to obtain the resulting classification. Each step corresponds to the number in the parenthesis of the workflow in Figure 2.

The RADAR images we used were obtained from ESA's Copernicus Hub, which allows open access to various Sentinel data assets. The base image was downloaded as a compressed .zip file which includes metadata and various separate band intensities. The image was loaded on an SSD instead of a larger capacity HDD in order to improve read/write performance. This can be seen in Figure 3.
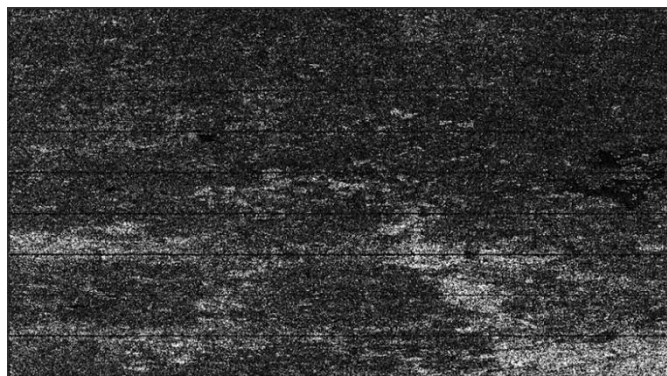

Figure 3: Raw Image Unprocessed VH polarity in SNAP

The image was split into its individual swath scans. This is done to allow us to narrow down to only the area in which we are interested in. Since these image files range anywhere from 100MB to 9GB in size, this is necessary for faster processing of the data. This is especially useful when performing analysis on off-the-shelf consumer grade hardware. The initial area was narrowed down to 2656 square kilometers from the full initial 8925 square kilometer area (Figure 4).

Figure 4: Sub-Selection of Area Swaths. The red square represents the 2 656km2 selection

We then applied radiometric calibration, which provides imagery in which pixel values can be directly related to scene backscattering [6], to ensure that downstream processes are not subject to additional noise or backscatter calibration errors.

De-burst: The image then undergoes a debursting process[5].This merges the individual scans and removes the swath lines which are the dark horizontal lines seen in Figure 3. To result in the image shown in Figure 5.
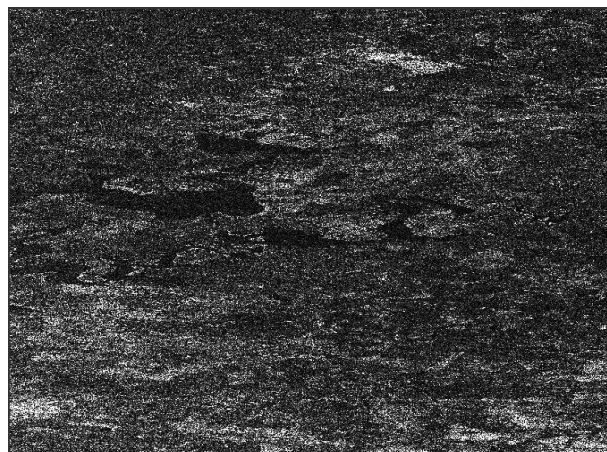

Figure 5: Image After Debursting (removing swath lines)

The resultant image (after debursting) was then further subdivided into an area measuring 25km by 75km resulting in an operating area of 1 875 square kilometers (Figure 6). Once again, this is done in order to be able to process the data in reasonable time on standard consumer devices. It is also not reasonable to expect that an area larger than this will be necessary for the current case.

Figure 6: Selection of reduced sub-swath study area.

A Frequency Domain Multilook (FDM)[5]was applied to the image. This divides the bandwidth of the image into several parts called Looks, each of which is used to form its own image. Combining these images results in an image

representation with a much greater Signal-to-noise Ratio (SNR) at the givenrange solution (Figure 7).
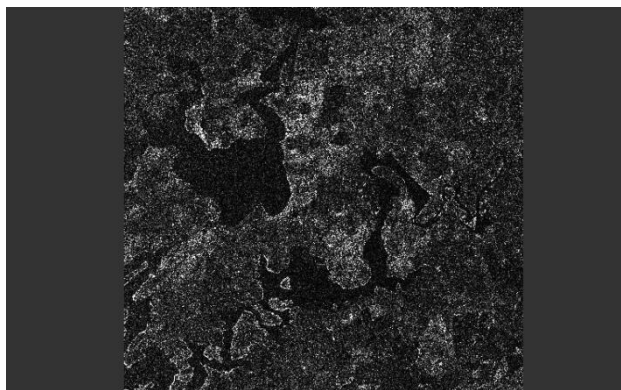

Figure 7: Final step resulting in the above multilook image.

At this point all the image preprocessing which is needed for decomposition is complete and the actual process of decomposition is started by creating a Polarimetric Matrix using SNAPs built in Polarimetric Matrix Generation[6] tool. This creates a matrix wherein each element of the matrix represents the backscatter response of the target in a particular polarization channel (Figure 8).
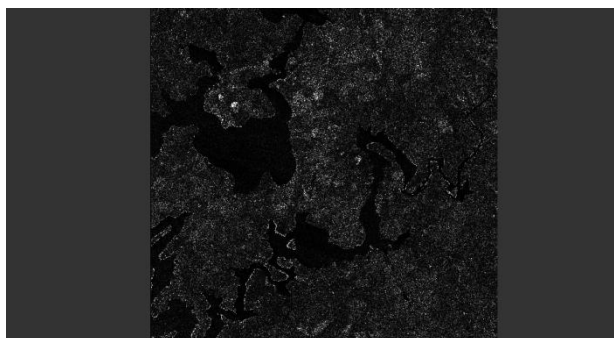

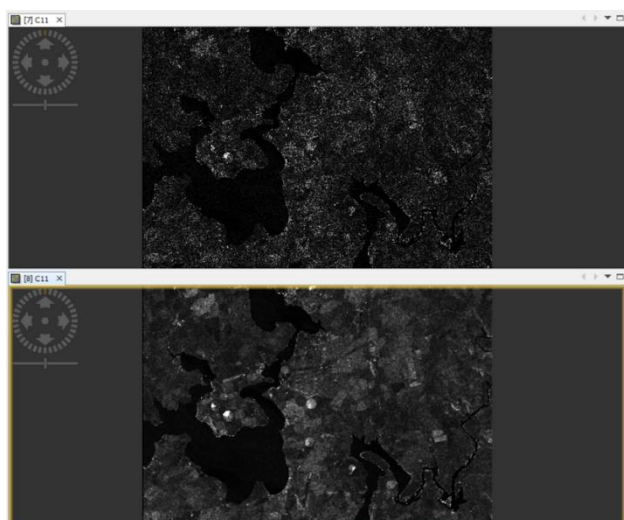Figure 8: Resulting Polarimetric Matrix image

Figure 9: Image after speckle filtering applied

Although the polarimetric matrix generation greatly reduced the SNR in the image, further speckle filtering is needed. A polarimetric speckle filter is hence applied. The effect of this can be seen in Figure 9 (note that it is taken at a smaller range solution). The Geometric Terrain correction was applied to the image to reduce the level of distortion present in any RADAR image. The resulting image has a much greater contrast for differentiating water bodies and other resolvable features at this range solution (Figure 10).
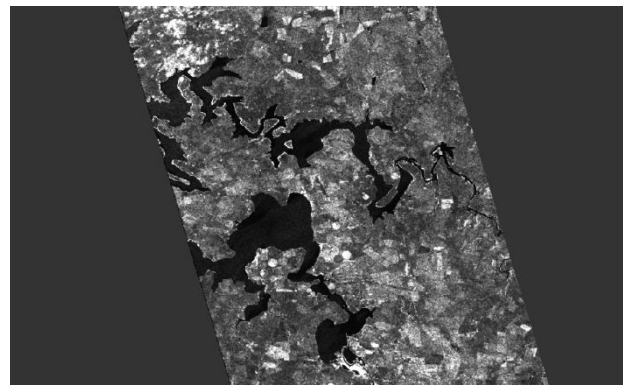

Figure 10: Correctly orientated image after geometric terrain correction

The final step in the decomposition process is the Polarimetric Decomposition[6]. This breaks down the image into Entropic, Anisotropic and Alpha decompositions (Figure 11).
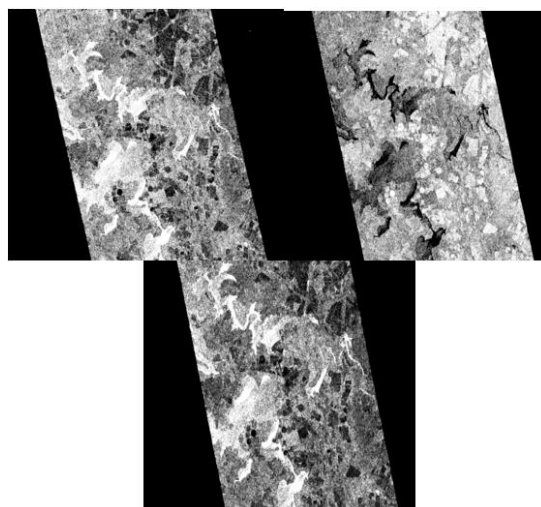

Figure 11: Entropic (top left), Anisotropic (top right) and Alpha (bottom) polarizations
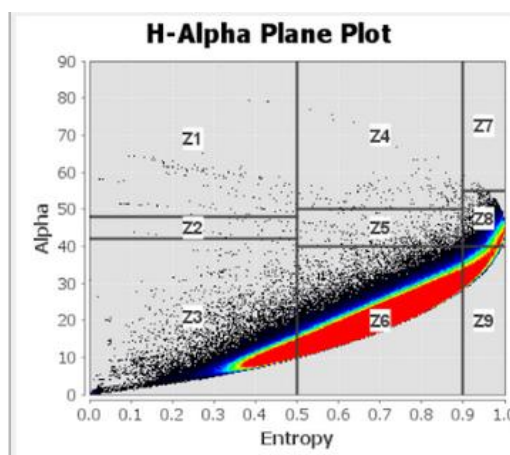

Figure 12: H-Alpha (Alpha vs Entropy) density plot

Once an image has been polarimetrically decomposed, the H-α decomposition can be visualized on an Entropy vs Alpha plot (Figure 12).This is a measure of a specific deep-red visible spectral line in the Balmer series [7].

At this point we run a Polarimetric Unsupervised Classification (PUC)[6] on the study area. This assignscolour codes to regions according to their polarization and radiometric intensity (Figure 13). It is used to differentiate and mark terrain properties but as an unsupervised method, it is still necessary to manually compare and identify them.
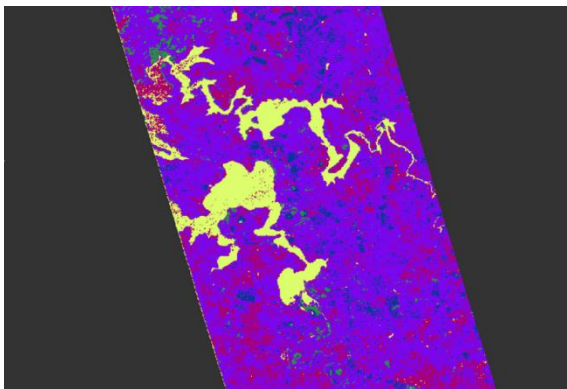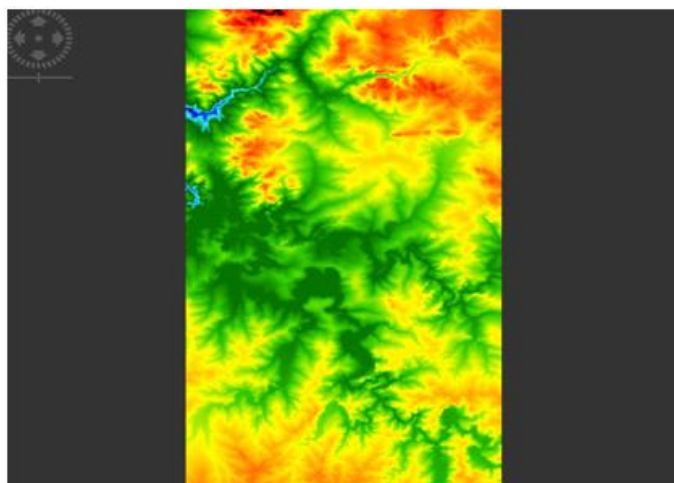
Figure 13: Resulting Classification colour map

We add context to the classified image by exporting it as a Keyhole Markup Language (.kmz) file and overlaying it onto the original region in Google Earth. The classifications assigned by the PUC are then identified by switching between true colour and the PUC and making inferences as to the terrain type based on known or observable references in the true colour image (Figure 14).
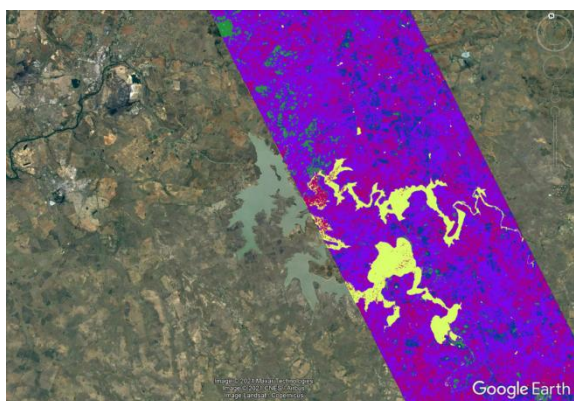

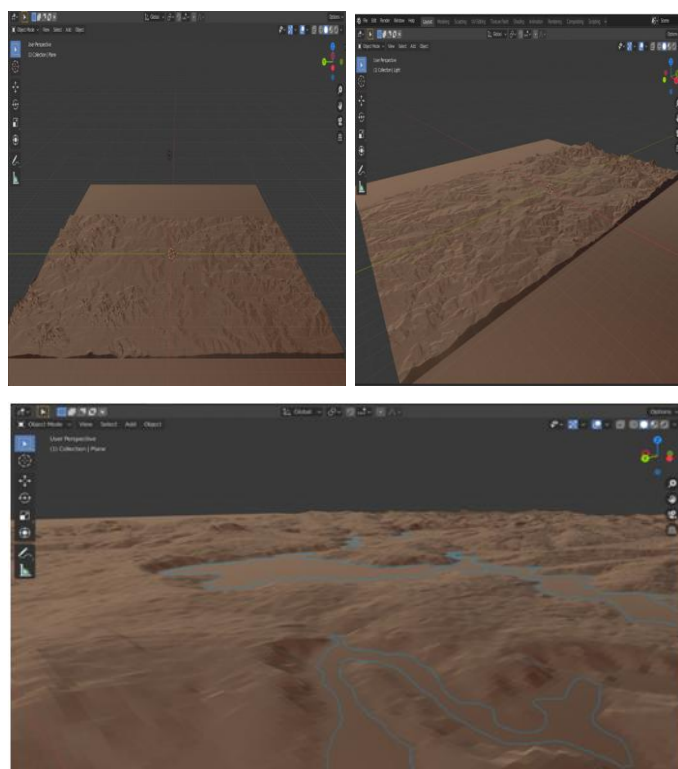Figure 14: classification colour overlayed in Google Earth

III. RESULTS

A. Table of Unsupervised Classification Results

Class	Colour	Frequency*	Description
Urban/ Impervious	#C0C0C0	0.614%	Complex Structures
Dense Vegetation	#01FF00	4.47%	Anisotropic Particles
Water	#FFFF00	5.49%	Anisotropic Scatter
Crops	#083897	5.59%	Bragg Surface
Bare Soil	#AC026F	19.68%	Non-Feasible Scattering
Sparse Vegetation	#6C2DC7	63.99%	Random Surface

*Frequency: the frequency is a proportional representation of the colour within the classified map. Only frequencies that appear in statistically significant proportions (> 0.1%) are labeled.

Figure 15: Elevation map generated in SNAP showing relative terrain heights

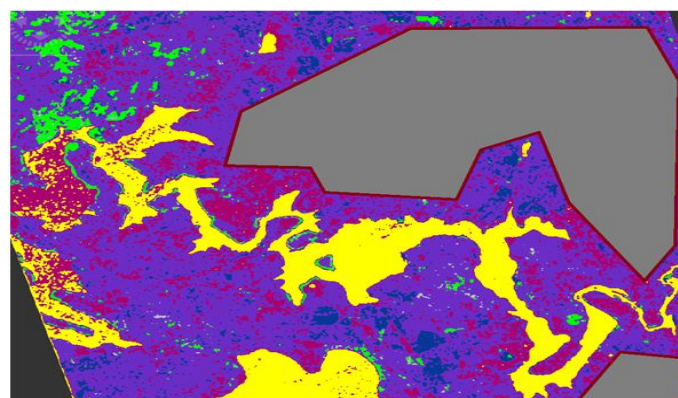Figure 16: 3D maps created in blender to aid in relative aspect visualization

Figure 17: Grey polygon showing suitable areas for future agricultural developments

IV. DISCUSSION

The final part of this report is an example of how the Wishart Classification and H-α decomposition of dual-polarization

polarimetric Synthetic Aperture Radar (SAR) data can be applied to applications such as the zoning of agricultural areas. This analysis involves identifying areas which would be suitable for agricultural zoning. These areas should adhere to the following arbitrary criteria:

- Within 1-5km of the main water body. This is within safe margin of the water table depth to ensure that there will always be water available when using boreholes or other pumped irrigation methods.
- No closer than 100 to 150m from the current water line. This is to mitigate flood risk.
- Elevation within 10m from the average dam level. This is to ensure a stable level of ground water retention and water availability.
- Slope must not have a gradient of more than 15 degrees. This is to reduce the rate of erosion over time as groundworks or crops are introduced.

The 3D terrain map (Figure 16) was made by exporting the elevation map as a greyscale image and converting it to a 3D terrain in Blender by applying it as a heightmap. 3D terrain mapping is useful in aiding decisions concerning certain terrain aspects such as slopes and hence the rate of erosion [8], although it should be noted that this information will need to be used in conjunction with soil samples and ground parameters as the rate of erosion in an area is greatly affected soil properties. The areassuitable for future agricultural developments were mostly classifiet as crops, bare soil and sparse vegetation.

CONCLUSION

It has been shown that the H-Alpha decomposition and Wishart classification technique is a suitable method in the case for determining suitable land for agriculture use and can be generalized to other land cover types in a similar manner [9]. It has been shown that this can be done with consumer grade hardware and using only FOSS software such as Google Earth and ESA'sSNAP as well as publicly available data from the Sentinel satellite constellation. The SNAP software has been shown to be capable of facilitating SAR image pre-processing, SAR image decomposition and SAR image classification and how this can be used in a practical application.

This technique is a valid approach to addressing the issues raised by growing urbanization and the need to expand agricultural output both in terms of crop supplyand crop exporting. Making use of SAR image classification can be considered a much less costly exercise than in-situ ground measurements as it can be done relatively easily and can cover much larger or inaccessible areas [9].

In summary, the H-alpha Wishart image decomposition and classification Polarimetric technique is a valid approach for uses such as agricultural planning and can easily be generalized to be used for urban mapping, town planning and erosion monitoring.

Conflicts of Interest: The authors declare no conflicts of interest

References

[1] European Space Agency 2022, SNAP, accessed 8 April 2021 https://step.esa.int/main/download/snap-download/

[2] Walls, Helen L., et al. "Understanding healthcare and population mobility in southern Africa: the case of South Africa." South African Medical Journal 106.1 (2016): 14-15.

[3] Kerrey, C:"Competing for land: The relationship between urban development and agriculture for lancaster and Seward Counties". 2012

[4] ESA 2014-2022 Copernicus Open Access Hub, accessed 26 April 2021, https://scihub.copernicus.eu/

[5] Donato A; Di Martino G; Iodice A, Riccio D and Ruello G: "RGB SAR products: methods and applications". European Journal of Remote Sensing, Volume 49, 2016 - Issue 1. 2016

[6] L. Veci: "SENTINEL-1 Toolbox, Polarimetric Tutorial", ESA; Skywatch 2019

[7] Seliakov, K. I., "Balmer lines in prominence spectra", Leningradskii Universitet Vestnik Matematika Mekhanika Astronomiia, pp. 134–139, 1975.

[8] Ontario, "Measuring Field Slopes to Estimate Soil Erosion," 13 02 2021. [Online]. Available: http://www.omafra.gov.on.ca/english/engineer/rusle2/fieldslope.htm. [Accessed 30 06 2021].

[9] Ran Yang, Jie Yang, and QianQing Qin "The application of H-α-Wishart on land cover classification and analysis", Proc. SPIE 7285, International Conference on Earth Observation Data Processing and Analysis (ICEODPA) 2008

Additional Reading

[10] K.E Trenberth:"Changes in precipitation with climate change", National Centre for Atmospheric and Oceanic Reseach, Vol. 47: 123–138, 2011

[11] Semenzato, A., "Mapping and Monitoring Urban Environment through Sentinel-1 SAR Data: A Case Study in the Veneto Region (Italy," International Journal of Geo-Information, vol. 9, no. 375, pp. 1-21, 2020.

[12] Davis-Reddy, C.L. and Vincent, K: Climate Risk and Vulnerability: A Handbook for Southern Africa (2nd Ed), CSIR, Pretoria, South Africa. 2017.